



# Carbon Monoxide Inhibits Porcine Reproductive and Respiratory Syndrome Virus Replication by the Cyclic GMP/Protein Kinase G and NF- $\kappa$ B Signaling Pathway

Angke Zhang,<sup>a,b</sup> Lijuan Zhao,<sup>a,b</sup> Na Li,<sup>a,b</sup> Hong Duan,<sup>a,b</sup> Hongliang Liu,<sup>a,b</sup> Fengxing Pu,<sup>a,b</sup> Gaiping Zhang,<sup>a,c</sup> En-Min Zhou,<sup>a,b</sup> Shuqi Xiao<sup>a,b</sup>

College of Veterinary Medicine, Northwest A&F University, Yangling, Shaanxi, China<sup>a</sup>; Experimental Station of Veterinary Pharmacology and Veterinary Biotechnology, Ministry of Agriculture, China, Yangling, Shaanxi, China<sup>b</sup>; College of Animal Science and Veterinary Medicine, Henan Agricultural University, Zhengzhou, Henan, China<sup>c</sup>

**ABSTRACT** Porcine reproductive and respiratory syndrome virus (PRRSV) causes significant economic losses to the pork industry worldwide each year. Our previous research demonstrated that heme oxygenase-1 (HO-1) can suppress PRRSV replication via an unknown molecular mechanism. In this study, inhibition of PRRSV replication was demonstrated to be mediated by carbon monoxide (CO), a downstream metabolite of HO-1. Using several approaches, we demonstrate that CO significantly inhibited PRRSV replication in both a PRRSV permissive cell line, MARC-145, and the predominant cell type targeted during *in vivo* PRRSV infection, porcine alveolar macrophages (PAMs). Our results showed that CO inhibited intercellular spread of PRRSV; however, it did not affect PRRSV entry into host cells. Furthermore, CO was found to suppress PRRSV replication via the activation of the cyclic GMP/protein kinase G (cGMP/PKG) signaling pathway. CO significantly inhibits PRRSV-induced NF- $\kappa$ B activation, a required step for PRRSV replication. Moreover, CO significantly reduced PRRSV-induced proinflammatory cytokine mRNA levels. In conclusion, the present study demonstrates that CO exerts its anti-PRRSV effect by activating the cellular cGMP/PKG signaling pathway and by negatively regulating cellular NF- $\kappa$ B signaling. These findings not only provide new insights into the molecular mechanism of HO-1 inhibition of PRRSV replication but also suggest potential new control measures for future PRRSV outbreaks.

**IMPORTANCE** PRRSV causes great economic losses each year to the swine industry worldwide. Carbon monoxide (CO), a metabolite of HO-1, has been shown to have antimicrobial and antiviral activities in infected cells. Our previous research demonstrated that HO-1 can suppress PRRSV replication. Here we show that endogenous CO produced through HO-1 catalysis mediates the antiviral effect of HO-1. CO inhibits PRRSV replication by activating the cellular cGMP/PKG signaling pathway and by negatively regulating cellular NF- $\kappa$ B signaling. These findings not only provide new insights into the molecular mechanism of HO-1 inhibition of PRRSV replication but also suggest potential new control measures for future PRRSV outbreaks.

**KEYWORDS** carbon monoxide, HO-1, NF- $\kappa$ B, PRRSV, cGMP/PKG

Porcine reproductive and respiratory syndrome (PRRS) is one of the most important infectious diseases impacting the swine industry worldwide and is characterized by reproductive failure in sows and respiratory diseases in pigs of all ages (1–3). PRRS is caused by porcine reproductive and respiratory syndrome virus (PRRSV), which is an

**Received** 14 September 2016 **Accepted** 12 October 2016

**Accepted manuscript posted online** 19 October 2016

**Citation** Zhang A, Zhao L, Li N, Duan H, Liu H, Pu F, Zhang G, Zhou E-M, Xiao S. 2017. Carbon monoxide inhibits porcine reproductive and respiratory syndrome virus replication by the cyclic GMP/protein kinase G and NF- $\kappa$ B signaling pathway. *J Virol* 91:e01866-16. <https://doi.org/10.1128/JVI.01866-16>.

**Editor** Stanley Perlman, University of Iowa

**Copyright** © 2016 American Society for Microbiology. All Rights Reserved.

Address correspondence to En-Min Zhou, [zhouem@nwsuaf.edu.cn](mailto:zhouem@nwsuaf.edu.cn), or Shuqi Xiao, [xiaoshuqi@nwsuaf.edu.cn](mailto:xiaoshuqi@nwsuaf.edu.cn).

A.Z. and L.Z. contributed equally to this article.

enveloped, single-stranded RNA virus belonging to the genus *Arterivirus*, family *Arteriviridae*, order *Nidovirales* (2). Present management strategies focus mainly on the prevention of infection through vaccination. Unfortunately, neither traditional control strategies nor conventional vaccines achieve consistent PRRS control (4–6). A major obstacle to successful PRRS vaccine development is the inconsistent induction of protective immunity (7–9). During PRRSV infection in animals, unknown viral properties apparently allow PRRSV to persist. Therefore, it is imperative to develop a safe and effective antiviral strategy to combat PRRSV infection.

Heme oxygenase-1 (HO-1), translated from HMOX1 mRNA, is a ubiquitously expressed, inducible isoform that catalyzes the first enzymatic rate-limiting step in heme degradation. HO-1 has numerous biological functions, including antioxidant, anti-inflammatory, antiapoptotic, and antiproliferative properties and plays an important role in host defense against microbial infection (10). Enhanced HO-1 expression inhibits replication of many viruses, including HIV-1, Ebola virus, hepatitis B virus (HBV), and hepatitis C virus (HCV) (11–14). Our previous work showed that overexpression or induction of HO-1 expression inhibits PRRSV and bovine viral diarrhea virus (BVDV) replication (15, 16). Furthermore, microRNA miR-24-3p promotes PRRSV replication through suppression of HO-1 expression (17), indicating that increased expression of HO-1 may provide a potential new antiviral strategy against PRRSV infection. However, the molecular mechanism of HO-1 inhibition of PRRSV replication remains unknown.

The physical protection properties of HO-1 are controlled, in part, by one or more downstream products of heme catabolism, including carbon monoxide (CO), biliverdin, and iron. CO, an endogenous messenger generated by HO-1 activity (18), can freely diffuse through and traverse all membranes. In recent years, CO has been verified to, within a range of concentrations, exert interesting biological activities, including anti-inflammatory, antiapoptotic, and cytoprotective actions in various disease models (19–22). These studies demonstrate beneficial effects of HO-1 and its products during different physiological and pathological processes. Although CO is known to be toxic and lethal in high concentrations, research is increasingly focused on revealing the role of CO as a signaling and regulatory molecule in many ongoing cellular processes (23). It has been demonstrated that CO mediates the antiviral effect of HO-1 during enterovirus infection (24). Moreover, a CO-releasing molecule (CORM-3) was found to exert bactericidal activity to inhibit *Pseudomonas aeruginosa* infection in an animal bacteremia model (25). In addition, CO inhibited the growth of both *Escherichia coli* and *Staphylococcus aureus* (26). Accumulating studies suggest therapeutic efficacy for CO inhalation therapies for certain disorders, due to the potent antioxidant, anti-inflammatory, and antiapoptotic activities of CO (27, 28). Most CO action has been reported to depend on the activation of soluble guanylate cyclase (sGC) and on subsequent increases in cellular levels of cyclic GMP (cGMP) (29–31), although the mechanisms downstream from cGMP production remain incompletely understood. Growing evidence supports a role for protein kinase G (PKG) as an important cGMP target that promotes cGMP effects in cardiac myocytes (32).

In this study, we used CO-releasing molecule II (CORM-2) to investigate the effect of the HO-1 downstream metabolite CO on PRRSV infection and to study molecular mechanisms that result in antiviral CO effects. We found that CO markedly inhibits PRRSV replication by activating the cellular cGMP/PKG signaling pathway and by negatively regulating cellular NF- $\kappa$ B signaling. These findings should provide new insights into the molecular mechanism effecting HO-1 inhibition of PRRSV replication and also guide development of potential new PRRSV control measures.

## RESULTS

**PRRSV infection promotes CO production.** To investigate whether PRRSV infection could induce CO production, MARC-145 cells were infected with PRRSV at different MOIs and at different time points. Cells were then incubated in the presence of 50  $\mu$ g/ml hemoglobin (Hb) for 24 h to quantify carboxyhemoglobin (HbCO) levels by ELISA as a measure of CO production. ELISA results showed that compared to uninfected cells,

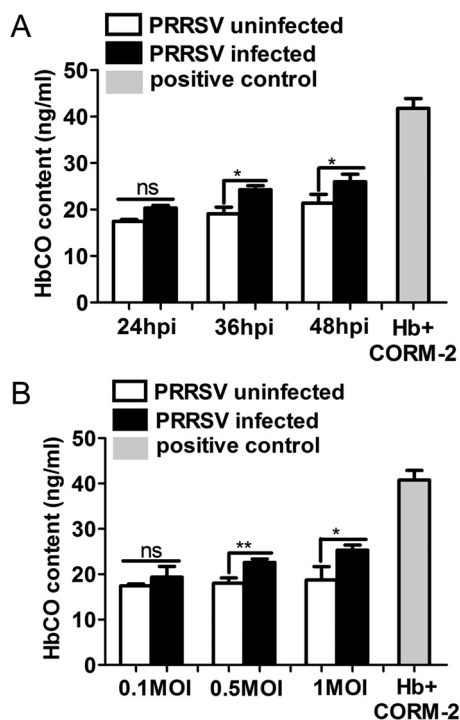


**FIG 1** PRRSV infection promotes CO production. (A) MARC-145 cells infected with PRRSV at an MOI of 0.1 were treated with Hb (50  $\mu$ g/ml) from 1 hpi onward. At 24, 36, and 48 hpi, cell culture supernatants were harvested for HbCO detection by ELISA to quantify HbCO levels as a measure of CO. MARC-145 cells mock infected with PRRSV were included as a control. (B) MARC-145 cells were infected with different doses of PRRSV (MOIs, 0.1, 0.5, and 1), and then the cells were incubated with 50  $\mu$ g/ml Hb for 24 h. The HbCO contents in culture supernatants were determined by ELISA as a measure of CO. Uninfected MARC-145 cells were included in the analysis as a control. Hb (50  $\mu$ g/ml) was coincubated with CORM-2 (150  $\mu$ M) for 1 h, and then the contents of HbCO were detected simultaneously as a positive control (A and B). Data are expressed as the means  $\pm$  standard deviations (SD) of the results of three independent experiments. *P* values were calculated using Student's *t* test. \*, *P* < 0.05; \*\*, *P* < 0.01; ns, not significant. White columns represent PRRSV-mock-infected MARC-145 cells, black columns represent PRRSV-infected MARC-145 cells, and gray columns represent the positive control.

PRRSV-infected cells showed increased HbCO content at 24, 36, and 48 h postinfection (hpi) (Fig. 1A). Moreover, PRRSV increased HbCO production in a dose-dependent manner (Fig. 1B). These results indicate that PRRSV infection could induce CO production in host cells.

#### Endogenous CO produced by HO-1 catalysis mediates the HO-1 antiviral effect.

Our previous research showed that HO-1 can suppress PRRSV replication (15, 17). However, the molecular mechanism of HO-1 inhibition of PRRSV replication is unclear. To explore this antiviral mechanism, we first investigated the effect of endogenous CO catalyzed by HO-1 upregulation on PRRSV infection. The major source of CO *in vivo* is the degradation of heme by HO-1. Hb can be used as an effective CO scavenger (24, 33), since it has very high affinity for CO. MARC-145 cells were pretreated with the CO scavenger Hb (50  $\mu$ g/ml) for 1 h; after the cells were washed with phosphate-buffered saline (PBS) three times, they were infected with PRRSV at an MOI of 0.1. One hour later, the virus solution was discarded and cells were treated with protoporphyrin IX cobalt chloride (CoPP) (80  $\mu$ M) in the presence or absence of 50  $\mu$ g/ml Hb. At 24 hpi, the cells and supernatants were harvested for further analysis. As shown in Fig. 2A, treatment with Hb markedly reversed the inhibitory effect of HO-1 on viral ORF7 mRNA expression, as exhibited by a 92% increase in ORF7 expression relative to that of the CoPP-only treatment group. Similar results were observed when PRRSV N protein expression levels in cells were analyzed (Fig. 2B). Treatment with Hb also resulted in markedly increased PRRSV RNA levels, which were 49% (Fig. 2C) higher than those of the CoPP-only control, with a concomitant 0.25-log increase in supernatant virus copies compared to that of

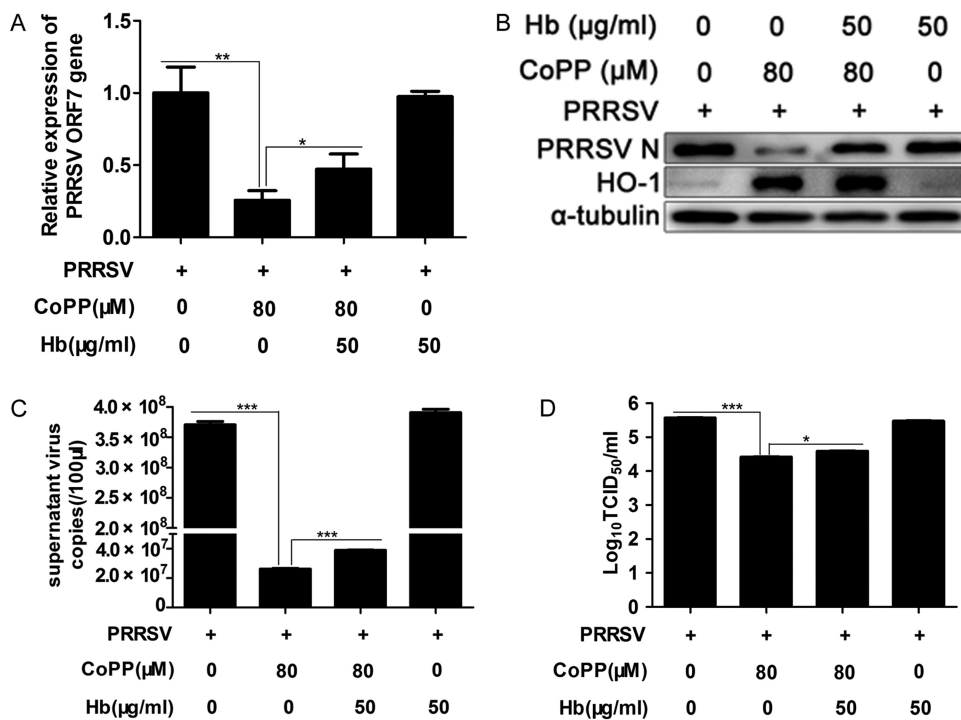


**FIG 2** CO produced by HO-1 catalysis mediates the inhibitory effect of HO-1 on PRRSV replication. MARC-145 cells were pretreated with the CO scavenger Hb (50  $\mu$ g/ml) for 1 h, and after being washed with PBS three times, the cells were infected with PRRSV at an MOI of 0.1. One hour later, the virus solution was discarded and the cells were treated with 80  $\mu$ M CoPP in the presence or absence of 50  $\mu$ g/ml Hb. At 24 hpi, PRRSV ORF7 mRNA (A), N protein (B), extracellular viral RNA (C), and progeny virus production (D) were determined using qPCR, Western blotting, and TCID<sub>50</sub> assay. Data are expressed as the means  $\pm$  SD of the results of three independent experiments. *P* values were calculated using Student's *t* test. \*, *P* < 0.05; \*\*, *P* < 0.01; \*\*\*, *P* < 0.001.

the control group (Fig. 2D). Therefore, Hb treatment partially reversed HO-1 inhibition of PRRSV infection. However, Hb treatment alone had no obvious effect on PRRSV infection. These results indicate that endogenous CO produced by HO-1 catalysis could reduce PRRSV replication.

**CORM-2 inhibits PRRSV replication in MARC-145 cells in a dose-dependent and time duration manner.** We used an exogenous CO donor, CORM-2, to confirm the antiviral effect of CO. MARC-145 cells were treated with CORM-2 or inactive CORM-2 (iCORM-2) at different concentrations 1 h after PRRSV infection. Quantitative PCR (qPCR) and Western blotting were performed to determine the abundance of PRRSV ORF7 mRNA and N protein at the indicated times postinfection. As shown in Fig. 3A and B, treatment with CORM-2 resulted in a marked decrease in PRRSV ORF7 mRNA and N protein in a dose-dependent manner at 24, 36, and 48 hpi. We also detected intracellular and supernatant progeny virus production using the 50% tissue culture infective dose (TCID<sub>50</sub>). Consistent with intracellular ORF7 mRNA and N protein expression, CORM-2 treatment also decreased intracellular and supernatant virus titers in a dose-dependent manner in MARC-145 cells (Fig. 3C and D). To further explore whether CORM-2 could suppress PRRSV genome replication, NSP2 mRNA expression was determined by qPCR to reflect the PRRSV genome RNA level after CORM-2 treatment. qPCR results showed that CORM-2 inhibited PRRSV NSP2 mRNA expression in a concentration-dependent manner at 24, 36, and 48 hpi (Fig. 3E), indicating that CO suppressed PRRSV genome replication. However, iCORM-2, an inactive molecule which cannot release CO, had no significant effect on PRRSV infection and replication (Fig. 3A to E). These results suggest that CO specifically mediated the antiviral effect of CORM-2. Indirect immunofluorescence assay (IFA) results also demonstrated the inhibitory effect of CORM-2 on PRRSV replication in a dose-dependent manner (Fig. 3F).

To demonstrate whether CO could inhibit replication of different titers of PRRSV, a similar experiment as that described above was performed. MARC-145 cells were

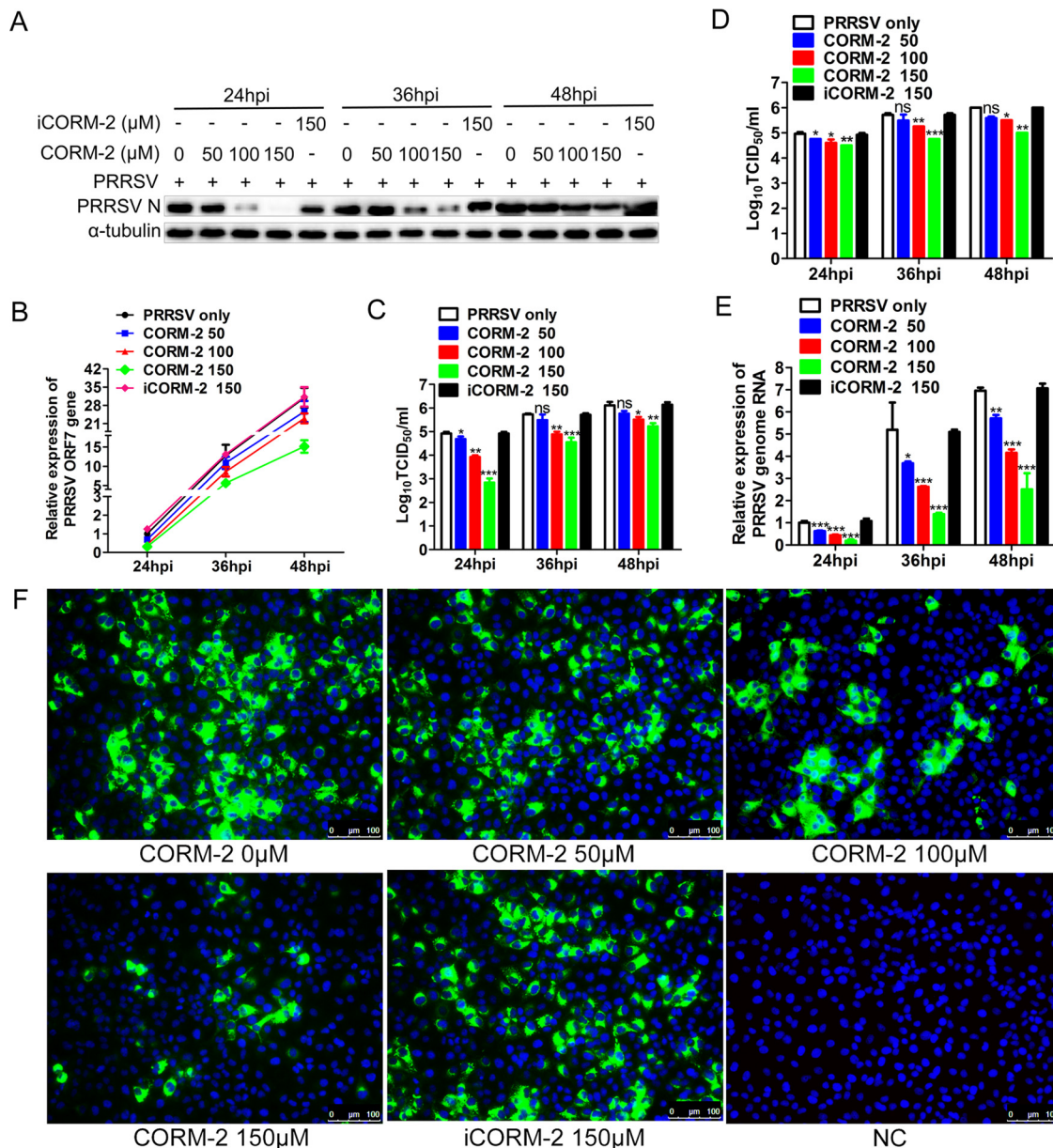


**FIG 3** CO inhibits PRRSV replication in MARC-145 cells in a dose-dependent and time duration manner. MARC-145 cells were infected with PRRSV at an MOI of 0.1, and then the cells were incubated with different concentrations of CORM-2 (50 to 150 μM) or iCORM-2 (150 μM) from 1 hpi onward. Cells and culture supernatants were collected at the indicated times; qPCR, Western blotting, and TCID<sub>50</sub> assay were performed to determine the levels of viral ORF7 mRNA (B), N protein (A), and intracellular (C) and supernatant (D) virus production. After treatment as described above, cells were harvested at 24, 36, and 48 hpi, respectively. (E) Relative levels of PRRSV RNA were detected with qPCR, using PRRSV NSP2-specific primers; (F) the expression of N protein was determined by IFA at 24 hpi, with MARC-145 cells mock infected with PRRSV included as a control (NC). Data are expressed as the means ± SD of the results of three independent experiments. *P* values were calculated using analysis of variance (ANOVA). \*, *P* < 0.05; \*\*, *P* < 0.01; \*\*\*, *P* < 0.001.

infected with PRRSV at different MOIs and then treated with CORM-2 or iCORM-2 for 24 h. As shown in Fig. 4A and B, CORM-2 treatment of MARC-145 cells significantly decreased the expression levels of intracellular PRRSV N protein and virus titers in the supernatants at different PRRSV MOIs; however, iCORM-2 did not have an obvious inhibitory effect on PRRSV infection. To confirm whether the inhibitory effect of CORM-2 on PRRSV replication is strain dependent, the other two PRRSV strains, JXA1 and VR2332, were used to infect MARC-145 cells at an MOI of 0.1. At 24 hpi, Western blot and titration assays were performed. Results showed that CO could decrease the expression level of N protein and virus titers of the different PRRSV strains, while iCORM-2 had no significant effect on PRRSV replication (Fig. 4C and D).

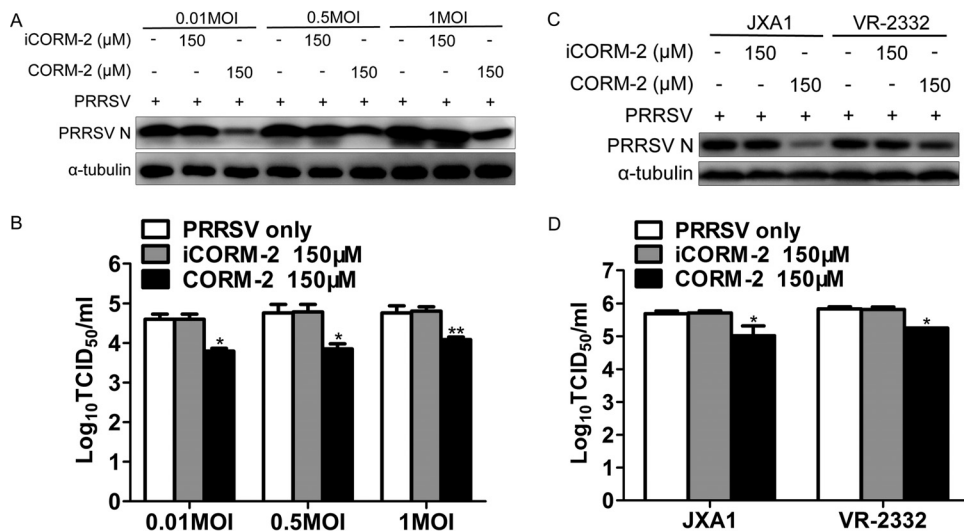


**FIG 4** The inhibition of viral replication by CO in MARC-145 cells is PRRSV titer and strain independent. (A and B) MARC-145 cells were infected with PRRSV at an MOI of either 0.01, 0.5, or 1 for 1 h and then treated with either CORM-2 (150 μM) or iCORM-2 (150 μM) for 24 h. The expression of intracellular PRRSV N protein and virus titers in supernatants were assayed by Western blotting (A) and TCID<sub>50</sub> determination (B), respectively. (C and D) MARC-145 cells were incubated with either JXA1 or VR-2332, each at an MOI of 0.1, for 1 h, followed by treatment with a 150 μM concentration of either CORM-2 or iCORM-2. The expression of intracellular PRRSV N protein and virus titers in the supernatants were assayed by Western blotting (C) and TCID<sub>50</sub> determination (D), respectively. Data are expressed as the means ± SD of the results of three independent experiments. *P* values were calculated using Student's *t* test. \*, *P* < 0.05; \*\*, *P* < 0.01.

**CO suppresses PRRSV replication in PAMs, and its anti-PRRSV activity is independent of HO-1 induction.** Since CO exerted potent antiviral activity in MARC-145 cells, we investigated whether CO also inhibits PRRSV replication in porcine alveolar macrophages (PAMs). PAMs were infected with PRRSV (MOI of 0.1), followed by treatment with various doses of CORM-2 or iCORM-2 from 1 hpi onward. At 24 hpi, cells and culture supernatants were harvested for further detection. Consistent with the results obtained in MARC-145 cells, CORM-2 treatment significantly reduced the expression levels of intracellular PRRSV ORF7 mRNA and PRRSV N protein, as well as virus titers in the supernatants, in a dose-dependent manner (Fig. 5A, B, and C). However, iCORM-2 treatment had no significant effect on PRRSV replication. According to our previous study, HO-1 acts as an antiviral factor in host cells. Therefore, here we further addressed whether the antiviral effect of CO was mediated by upregulation of HO-1 as a positive feedback loop. qPCR (Fig. 5D) and Western blot (Fig. 5E and F) results showed that CORM-2 or iCORM-2 treatment showed no marked effect on HO-1 mRNA and protein expression compared with that of the control group in both MARC-145 cells and PAMs. These results indicate that CO inhibition of PRRSV infection may not be mediated by HO-1 upregulation.

**CO does not affect virus entry of the PRRSV life cycle.** To investigate whether CO affects virus entry of the PRRSV life cycle, the kinetics of the antiviral activity of CO against PRRSV were analyzed with time-of-addition assays. The results showed that CO did not have an obvious inhibitory effect on the progeny viral production and N protein expression when it was added immediately after the temperature shift (Fig. 6A and B). Consistent with these findings, no inhibitory effect was observed when CORM-2 was added at 2 h (Fig. 6C) or 4 h (Fig. 6D) after the cells were shifted to 37°C. Taken together, these data indicate that CO did not block the viral entry process in MARC-145 cells. So, we further explored whether CO inhibited the spread of PRRSV in host cells.

**CO inhibits PRRSV intercellular spread.** To determine whether CO affects the transfer of infection between cells, PRRSV spread in the presence of PRRSV-neutralizing antibodies and CORM-2 was analyzed in the following experiments. First, a standard virus-neutralizing assay was performed to determine the neutralizing antibody titer of

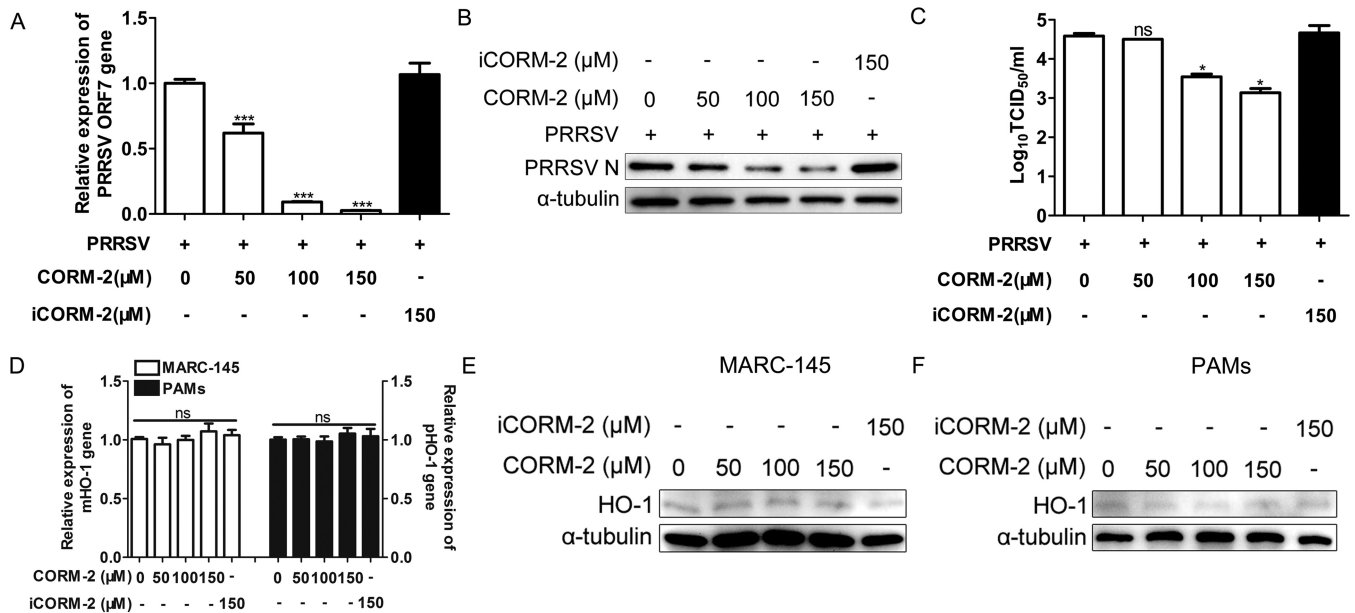


**FIG 5** CO suppresses PRRSV replication in PAMs, and its anti-PRRSV activity is independent of HO-1 induction. (A to C) PAMs were infected with PRRSV at an MOI of 0.1 for 1 h and then incubated in the presence or absence of the indicated concentrations of CORM-2 (50 to 150 μM) or iCORM-2 (150 μM) for 24 h. The levels of ORF7 mRNA (A), N protein (B), and virus titers (C) were assayed by qPCR, Western blotting, and TCID<sub>50</sub> determination, respectively. (D to F) MARC-145 cells or PAMs were treated with various concentrations of CORM-2 (50 to 150 μM) or iCORM-2 (150 μM) for 24 h. The cells were then harvested, and the abundance of HO-1 mRNA was determined by qPCR (D) and the expression of HO-1 protein was detected by Western blotting (E and F). Data are expressed as the means ± SD of the results of three independent experiments. *P* values were calculated using ANOVA. \*, *P* < 0.05; \*\*\*, *P* < 0.001; ns: not significant.

a swine hyperimmune serum sample. Simultaneously, a negative serum sample from an uninfected pig at the same dilution was included as a control. Virus-neutralizing assay results showed that the swine hyperimmune serum at a titer of 1:8 completely blocked PRRSV infection, indicating that this serum blocked the initial virus entry into the host cells; however, the negative serum did not have the same effect (Fig. 7A). To determine whether CO could block PRRSV intercellular spread, MARC-145 cells infected with PRRSV were incubated in the presence of 1:8 swine hyperimmune serum together with

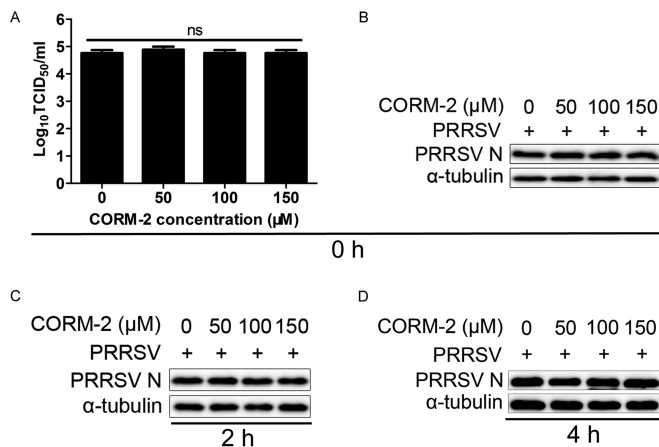


**FIG 6** CO does not affect virus entry of the PRRSV life cycle. In the entry assay, the kinetics of the antiviral activity of CO against PRRSV were evaluated with time-of-addition assays. Cells were challenged with PRRSV (MOI of 0.1) for 3 h at 4°C and then incubated at 37°C in the presence of CORM-2 for 6 h. CORM-2 was added at 0, 2, or 4 h (the time point at which the cells were switched to 37°C was set to 0 h). The cells were then rinsed and incubated for another 24 h at 37°C. The inhibitory effects were determined when CORM-2 was added at 0 (A and B), 2 (C), or 4 h (D) after the cells were shifted to 37°C. Data are expressed as the means ± standard deviations of the results of three independent experiments. *P* values were calculated using ANOVA. ns, not significant.

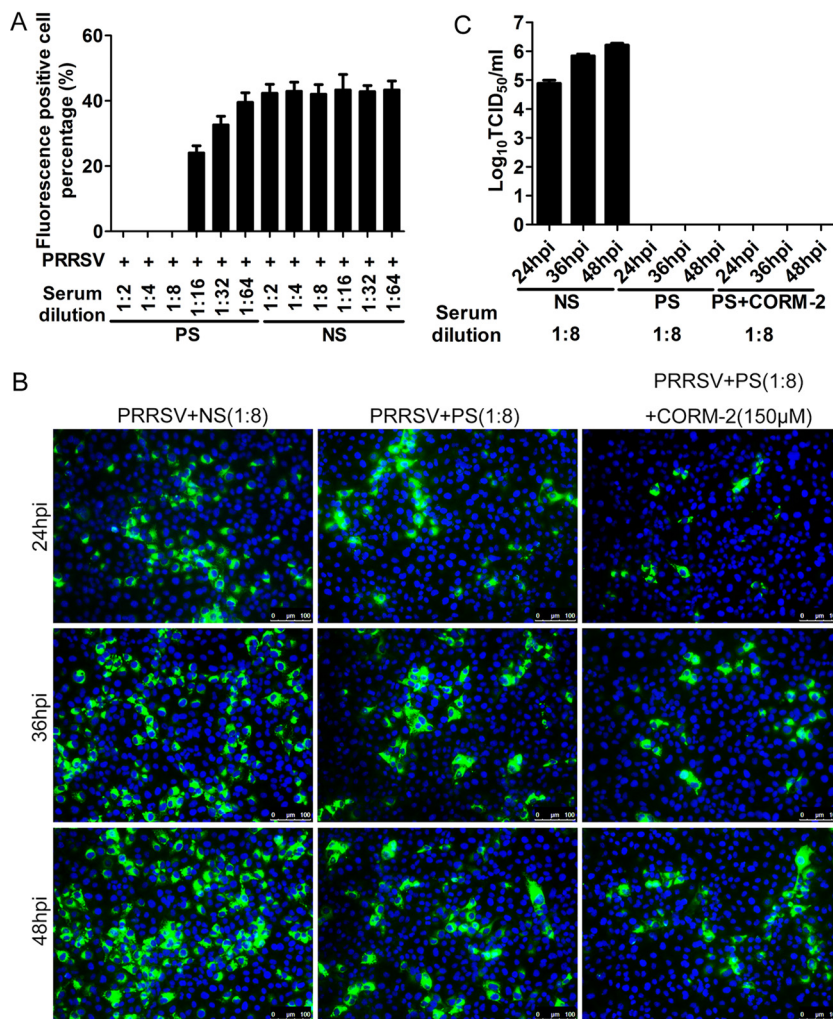


**FIG 7** CO inhibits PRRSV intercellular spread. (A) Standard virus-neutralizing assay. Hyperimmune serum from a PRRSV-infected pig was serially diluted and incubated with the virus for 1 h at 37°C; the virus-antibody complex was then added to the MARC-145 cells. At 24 hpi, the cells were stained with 6D10, and fluorescence-positive cells were counted under the fluorescence microscope. The percentage of fluorescence-positive cells was calculated. (B) CO suppresses the intercellular spread of PRRSV. MARC-145 cells were infected with PRRSV at an MOI of 0.1. At 3 hpi, the negative serum, a 1:8 dilution of the hyperimmune serum, or a 1:8 dilution of the hyperimmune serum plus CORM-2 (150 µM) was added to the infected cells. At 24, 36, or 48 hpi, IFA was performed to detect the expression of N protein. (C) Virus titers of culture supernatants from the experiment described for panel B. The virus titer of culture supernatants was determined by TCID<sub>50</sub> assay. NS, negative-control serum from an uninfected pig; PS, hyperimmune serum from a PRRSV-infected pig.

CORM-2 (150 µM) from 3 hpi onward. At 24, 36, and 48 h after PRRSV infection, IFA was performed to detect the expression of PRRSV N protein. IFA results showed that PRRSV infection was obviously blocked in the presence of 1:8 swine hyperimmune serum, indicating that virus-neutralizing serum prevents cell-free diffusion of virus. Based on this effect of virus-neutralizing serum, a few small foci were observed at 24 hpi in the virus-neutralizing serum group; larger foci were observed at 36 and 48 hpi in the same group, indicating that the viruses were continuing to spread from cell to cell in the presence of neutralizing serum (Fig. 7B). However, foci observed in virus-neutralizing serum plus CORM-2 group at 24, 36, and 48 hpi were smaller than those in the corresponding neutralizing serum group at the same time points, respectively (Fig. 7B). These results indicate that CO effectively inhibits PRRSV intercellular spread. To confirm that neutralizing antibody remained through the time course, cell culture supernatants were inoculated onto MARC-145 cells in 96-well plates for virus titer detection. Culture



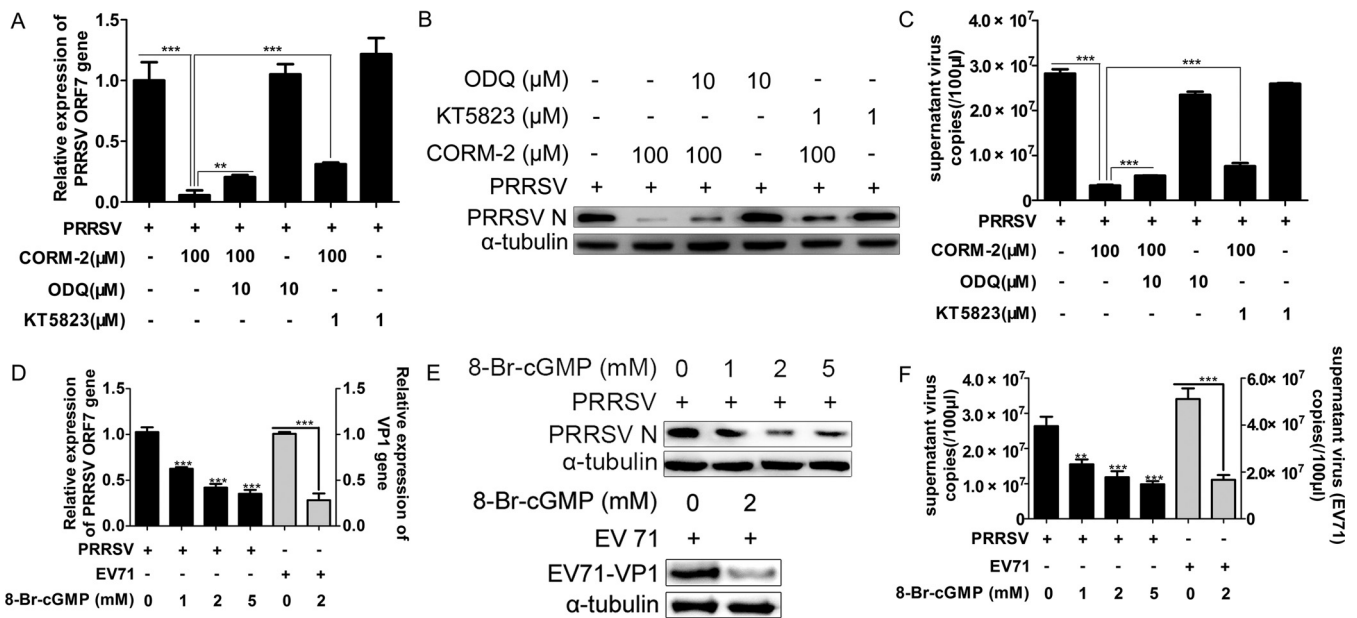


**FIG 8** CO inhibits PRRSV replication mediated via the cGMP/PKG signaling pathway. (A to C) MARC-145 cells were infected with PRRSV at an MOI of 0.1 for 1 h, and cells were then treated with either ODQ (10  $\mu$ M) or KT5823 (1  $\mu$ M) in the presence or absence of 100  $\mu$ M CORM-2 for 36 h. The abundance of intracellular ORF7 mRNA and supernatant viral RNA copy numbers were analyzed by qPCR (A and C). Expression of N protein was determined by Western blotting (B). (D to F) MARC-145 cells were treated with various doses of 8-Br-cGMP (1, 2, 5 mM) from 1 hpi onward. Cells and culture supernatants were harvested at 36 hpi for further analysis. PRRSV replication was determined using qPCR for intracellular ORF7 mRNA (D) and supernatant virus copy numbers (F) and Western blotting for PRRSV N protein (E). SK-N-SH cells infected with EV71 (MOI of 0.1) were treated with 2 mM 8-Br-cGMP from 1 hpi onward. Cells were harvested at 24 hpi, and then EV71 VP1 mRNA (D) and supernatant progeny virus production (F) and VP1 protein expression (E) were determined by qPCR and Western blotting, respectively. Data are expressed as the means  $\pm$  SD of the results of three independent experiments. *P* values were calculated using Student's *t* test. \*\*, *P* < 0.01; \*\*\*, *P* < 0.001.

supernatants containing swine hyperimmune serum did not generate any infections, while parallel control supernatants containing negative serum generated infection, and the virus titer increased gradually with the advance of the infection time (Fig. 7C).

**CO suppression of PRRSV replication via cGMP/PKG signaling pathway activation.** To investigate whether the cGMP/PKG-mediated signaling pathway is involved in the protective effect of CO against PRRSV infection, PRRSV-infected MARC-145 cells were coincubated with CORM-2 and either the soluble guanylate cyclase (sGC) inhibitor 1*H*-[1,2,4]oxadiazolo[4,3- $\alpha$ ]quinoxalin-1-one (ODQ) or the protein kinase G (PKG) inhibitor KT5823. qPCR and Western blot analyses were performed at 36 hpi to detect the expression of intracellular PRRSV ORF7 mRNA, N protein, and virus copies in the supernatants. The results show that treatment with either ODQ or KT5823 partially reversed the CORM-2-induced reduction of intracellular viral RNA, protein expression, and extracellular viral RNA (Fig. 8A to C). However, ODQ or KT5823 treatment alone exerted no significant effects on PRRSV replication. Next, we mimicked sGC activation by incubating the cells with the cell-permeable cGMP analog 8-Br-cGMP to confirm the cGMP-mediated inhibitory effect on PRRSV replication. MARC-145 cells were treated with various doses of 8-Br-cGMP (1, 2, and 5 mM) from 1 hpi onward. Cells and culture supernatants were harvested at 36 hpi for further analysis. As shown in Fig. 8D to F, 8-Br-cGMP dose dependently decreased the expression of intracellular PRRSV ORF7 mRNA, N protein, and virus copies in the supernatants. To further confirm the activity of the cGMP analog 8-Br-cGMP, the effect of 8-Br-cGMP on enterovirus 71 (EV71) infection in SK-N-SH cells was determined simultaneously as a positive control according to previous reports (24). SK-N-SH cells infected with EV71 (MOI of 0.1) were treated with 2 mM 8-Br-cGMP from 1 hpi onward. Cells were harvested at 24 hpi, and EV71 VP1 mRNA level, protein expression, and supernatant virus copies were determined by qPCR and Western blot analyses. qPCR and Western blot results showed that 8-Br-cGMP significantly inhibited the abundance of EV71 VP1 mRNA (Fig. 8D) and supernatant progeny virus copies (Fig. 8F), as well as the expression of VP1 protein (Fig. 8E).

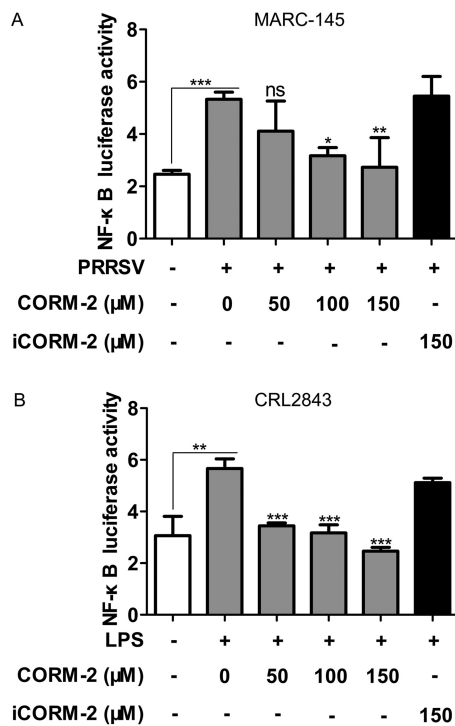


**FIG 9** CO inhibits NF- $\kappa$ B-responsive promoter activity. MARC-145 and CRL2843 cells were transfected with 100 ng/well of pNF- $\kappa$ B-Luc and 50 ng/well of pRL-TK. (A) At 12 h posttransfection, MARC-145 cells were infected with PRRSV at an MOI of 0.1, followed by treatment with various concentrations of CORM-2 or 150  $\mu\text{M}$  iCORM-2 from 1 hpi onward; 36 h after PRRSV infection, cells were lysed for luciferase activity detection. (B) CRL2843 cells were treated with LPS in the presence of various doses of CORM-2 or 150  $\mu\text{M}$  iCORM-2 12 h after transfection. After treatment with LPS for 36 h, the cells were lysed and luciferase activity was measured. Data are expressed as the means  $\pm$  standard deviations of the results of four independent experiments; *P* values were calculated using ANOVA. \*, *P* < 0.05; \*\*, *P* < 0.01; \*\*\*, *P* < 0.001.

**CO interferes with NF- $\kappa$ B-responsive promoter activation.** To determine whether CO might impact PRRSV-induced NF- $\kappa$ B-responsive promoter activity, we constructed a luciferase reporter plasmid, pNF- $\kappa$ B-Luc, containing four NF- $\kappa$ B binding elements located upstream of a luciferase gene and then transiently transfected MARC-145 or CRL2843 cells, which was followed by treatment with various combinations of CORM-2, iCORM-2, PRRSV, and lipopolysaccharide (LPS). Exposure of cells to PRRSV increased luciferase activity, whereas treatment with CORM-2 significantly reduced PRRSV infection-induced NF- $\kappa$ B-responsive promoter activity in a concentration-dependent manner (Fig. 9A). Further, CORM-2 inhibited LPS-induced NF- $\kappa$ B-responsive promoter activity in CRL2843 cells (Fig. 9B), suggesting that CO might target the NF- $\kappa$ B pathway.

**CO blocks the NF- $\kappa$ B signaling pathway.** To investigate the mechanism of CO-mediated inhibition of NF- $\kappa$ B activation, we assessed several important control points of the NF- $\kappa$ B activation pathway, such as I $\kappa$ B- $\alpha$  phosphorylation upon PRRSV infection or LPS treatment. Western blot results showed that CORM-2 had no obvious effect on I $\kappa$ B- $\alpha$  degradation and phosphorylation in uninfected cells. In contrast, CORM-2 blocked PRRSV-induced I $\kappa$ B- $\alpha$  degradation and I $\kappa$ B- $\alpha$  phosphorylation in both MARC-145 cells and PAMs in a dose-dependent manner (Fig. 10A and B). However, iCORM-2 had no significant effect on PRRSV-induced I $\kappa$ B- $\alpha$  degradation and I $\kappa$ B- $\alpha$  phosphorylation. To further confirm that CO can suppress PRRSV-induced NF- $\kappa$ B activation, we evaluated the effect of CO on NF- $\kappa$ B subunit p65 translocation to the nucleus. Western blot analysis was performed to analyze the nuclear and cytosolic fractions of MARC-145 cells and PAMs. The p65 subunit of NF- $\kappa$ B was translocated into the nucleus after PRRSV infection either in the absence or presence of iCORM-2. However, treatment with CORM-2 markedly inhibited this translocation in a dose-dependent manner (Fig. 10C and D).

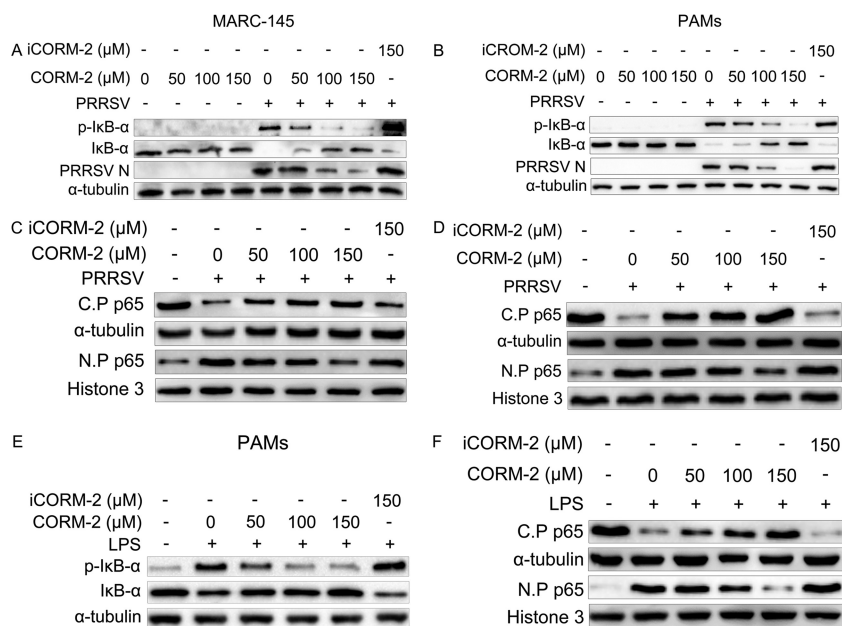


**FIG 10** CO inhibits PRRSV-induced NF- $\kappa$ B activation. (A and B) MARC-145 cells (A) or PAMs (B) were mock infected or infected with PRRSV (MOI of 0.1) in the presence of CORM-2 (50, 100, and 150  $\mu$ M) or iCORM-2 (150  $\mu$ M). At 36 hpi, the cells were harvested and I $\kappa$ B- $\alpha$ , p-I $\kappa$ B- $\alpha$ , and N protein were determined by Western blotting. (C and D) MARC-145 cells (C) or PAMs (D) were mock infected or infected with PRRSV (MOI of 0.1) in the presence or absence of CORM-2 (50, 100, and 150  $\mu$ M) or iCORM-2 (150  $\mu$ M) for 36 h. Total cell lysates were separated into nuclear protein (N.P) and cytoplasmic protein (C.P) fractions for detecting the distribution of p65. Histone 3 and  $\alpha$ -tubulin were used as nuclear and cytoplasmic controls, respectively. (E) PAMs were treated with LPS in the presence of CORM-2 (50, 100, and 150  $\mu$ M) or iCORM-2 (150  $\mu$ M) for 24 h. The cells were harvested, and I $\kappa$ B- $\alpha$  and p-I $\kappa$ B- $\alpha$  were determined by Western blotting. (F) PAMs were treated with LPS in the presence of CORM-2 (50, 100, and 150  $\mu$ M) or iCORM-2 (150  $\mu$ M) for 24 h. Total cell lysates were separated into nuclear protein and cytoplasmic protein fractions to detect the distribution of p65. Histone 3 and  $\alpha$ -tubulin were used as nuclear and cytoplasmic controls, respectively.

To exclude the possibility that the inhibitory effect of CO on NF- $\kappa$ B might result from CO inhibition of PRRSV N protein expression, we studied the activation of NF- $\kappa$ B through LPS stimulation. As shown in Fig. 10E and F, CO effectively prevented I $\kappa$ B- $\alpha$  degradation and phosphorylation in PAMs treated with LPS. Furthermore, in LPS-treated cells, NF- $\kappa$ B subunit p65 nuclear translocation was significantly decreased by CORM-2 treatment as well, suggesting that CO acts on the cellular NF- $\kappa$ B signaling pathway.

**The NF- $\kappa$ B signaling pathway participates in the inhibitory effect of CO on PRRSV replication.** To further investigate the relationship between CO, NF- $\kappa$ B, and PRRSV replication, we examined whether NF- $\kappa$ B was required for optimal PRRSV replication. MARC-145 cells or PAMs pretreated with the specific NF- $\kappa$ B inhibitor BAY11-7082 for 1 h before PRRSV infection exhibited markedly decreased intracellular PRRSV N protein expression levels and lower progeny PRRSV titers in experimental supernatants than controls pretreated with dimethyl sulfoxide (DMSO) alone (Fig. 11A to D). In supernatants, a 0.25- to 0.7- $\log_{10}$  reduction and a 0.45- to 0.75- $\log_{10}$  reduction in virus titers were observed in MARC-145 cells and PAMs, respectively, compared with the virus titers in DMSO-only pretreated controls (Fig. 11B and D).

**CO significantly reduces PRRSV-induced proinflammatory cytokine mRNA levels in MARC-145 cells or PAMs.** To determine whether treatment of MARC-145 cells or PAMs with CORM-2 affected the expression of proinflammatory cytokines induced by PRRSV infection, we assessed interleukin-6 (IL-6), IL-8, tumor necrosis factor alpha (TNF- $\alpha$ ), and IL-1 $\beta$  mRNA levels in both MARC-145 cells and PAMs using qPCR. As shown in Fig. 12A to H, CO significantly reduced the upregulation of IL-6, IL-8, TNF- $\alpha$ , and IL-1 $\beta$  mRNA levels induced by PRRSV infection at 24 hpi in a concentration-dependent manner, compared to that of mock-treated control groups.

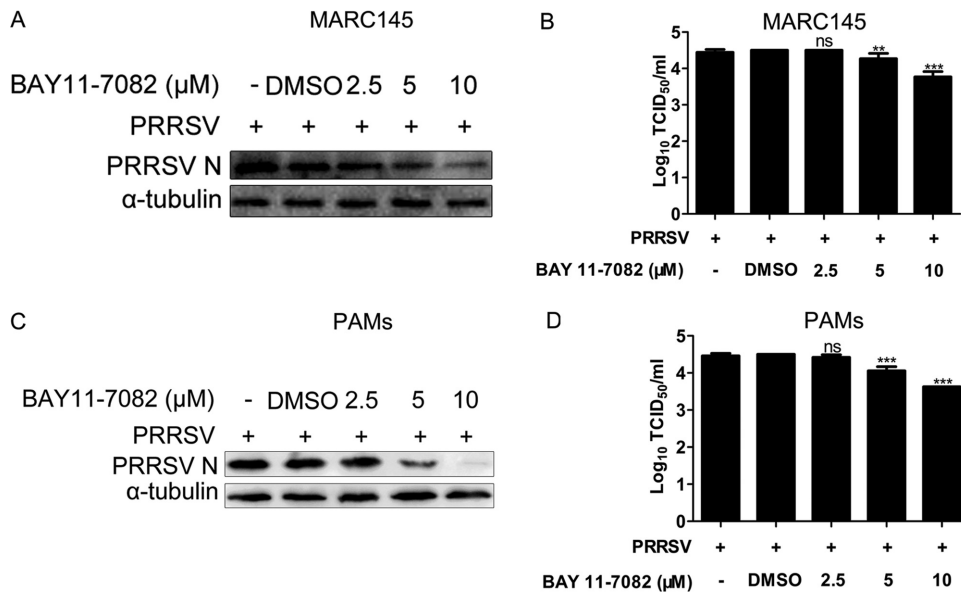


**FIG 11** Relationship between NF-κB activity and PRRSV replication. MARC-145 cells and PAMs were pretreated with BAY11-7082 or DMSO for 1 h prior to PRRSV infection. At 36 h postinfection, cells and supernatants were collected for Western blot detection of N protein and TCID<sub>50</sub> detection of progeny virus production. Data are expressed as the means ± standard deviations of the results of three independent experiments; *P* values were calculated using ANOVA. \*\*, *P* < 0.01; \*\*\*, *P* < 0.001.

**DISCUSSION**

Our previous study demonstrated that HO-1 could suppress PRRSV replication (15, 17). However, the molecular mechanisms of HO-1 inhibition of PRRSV replication are still unknown. Several studies have reported that one of the metabolites of HO-1, CO, exhibits anti-infection activity. CO has been shown to reduce the growth of *E. coli*, *P. aeruginosa*, and *S. aureus* (26, 34–36), and CO mediates the antiviral effect of HO-1 during EV71 infection (24). In this study, we investigated the effect of the HO-1 metabolite CO on PRRSV infection in MARC-145 cells or PAMs and its possible mechanism of action. Our results showed that CO mediates the anti-PRRSV activity of HO-1

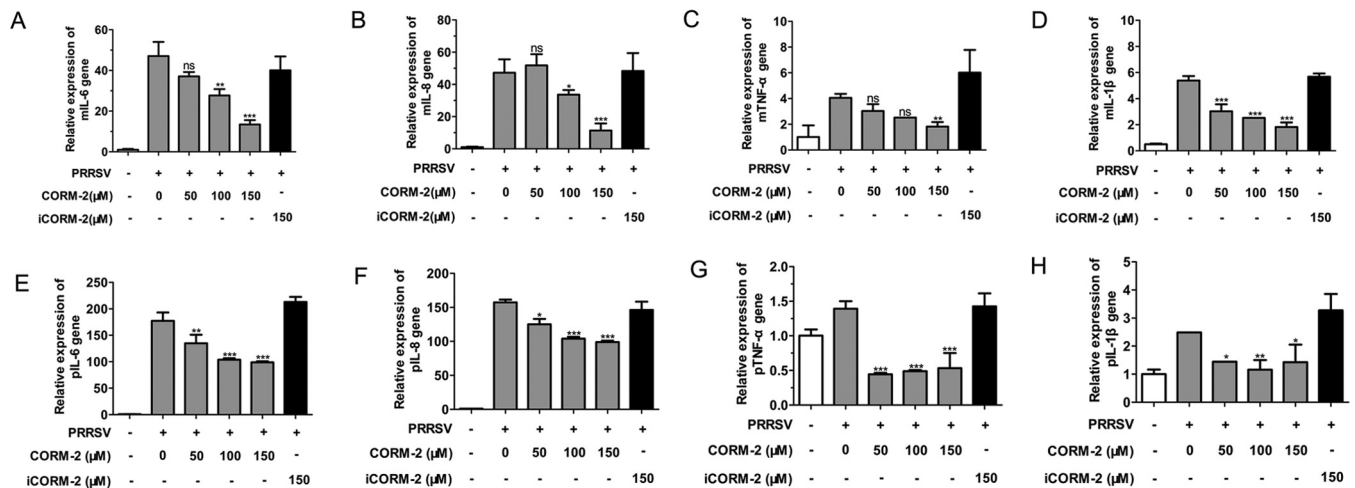


**FIG 12** CO reduces the inflammatory cytokine mRNA levels in PRRSV-infected MARC-145 cells and PAMs. (A to D) MARC-145 cells were infected with PRRSV (MOI of 0.1) and incubated in the presence or absence of various doses of CORM-2 or iCORM-2. Total RNA was extracted from cell lysates at 24 hpi. The relative expression levels of IL-6 mRNA (A), IL-8 mRNA (B), TNF-α mRNA (C), and IL-1β mRNA (D) were assessed by qPCR. Values were normalized to the internal control β-actin. (E to H) PAMs were treated as described above. The relative expression levels of IL-6 mRNA (E), IL-8 mRNA (F), TNF-α mRNA (G), and IL-1β mRNA (H) were each assessed by qPCR. Values were normalized to the internal control β-actin. The data are representative of three independent experiments performed in triplicate and are shown as the means ± SD. Statistical analysis was performed using ANOVA. \*, *P* < 0.05; \*\*, *P* < 0.01; \*\*\*, *P* < 0.001.

via the cGMP/PKG and NF- $\kappa$ B signaling pathway, thus expanding the cytoprotective role of the HO-CO system in the host cell response to virus invasion.

Endogenous production of CO occurs via enzymatic heme degradation by HO-1. According to our present research, PRRSV infection did not significantly induce HO-1 expression (Fig. 2B); however, it slightly promoted CO production (Fig. 1). These results suggest that PRRSV infection may stimulate CO production by increasing HO-1 activity but not its expression. Some reports showed that HO-1 and its downstream metabolite CO can regulate the immune function of host cells (37, 38). Therefore, we speculate that the PRRSV infection-induced HO-1 activity enhancement and subsequent CO increase may be an antiviral or innate immunity mechanism of host cells invaded by PRRSV. Though PRRSV infection could induce CO (Fig. 1), treatment with Hb alone did not markedly increase PRRSV infection (Fig. 2), indicating that the antiviral effect of endogenous CO is weak in PRRSV infection. However, based on our previous research and this study, inducing a large amount of HO-1 or overproducing CO in cells significantly inhibits PRRSV replication. These studies suggest that induction of HO-1 or CO may be a useful method to prevent or treat PRRSV infection.

CO has exhibited beneficial activities and holds promise as a therapeutic treatment when used at appropriate concentrations, as demonstrated in numerous animal disease models and *in vitro* experiments (21, 22). In the present study, we have provided solid evidence to identify a novel function for the HO-1/CO system as an effective antiviral pathway used by host cells to combat PRRSV infection. Our data indicate that CORM-2, an efficient CO release molecule, can greatly inhibit PRRSV replication in both MARC-145 cells and PAMs; however, iCORM-2 did not show the same effect (Fig. 3, 4, and 5), suggesting a CO-specific mediation of the CORM-2 antiviral effect. In addition, HO-1-derived CO also plays an important role in the anti-PRRSV cellular response, since the protective effect of HO-1 induction by CoPP was partly eliminated by the CO scavenger hemoglobin but mimicked by CORM-2 incubation (Fig. 2 and 3). After treatment with CORM-2, the expression of PRRSV N protein (Fig. 3A and F) and the intracellular virus titer (Fig. 3C) markedly decreased; in contrast, a moderate decline of supernatant progeny virus production was observed (Fig. 3D). Hence we speculated that CO may exert its antiviral activity mainly intracellularly and may consequently block the release of mature progeny virus particles.

As a gaseous second messenger, CO is attracting attention as a protective and homeostatic molecule with important signaling properties in physiological and pathophysiological situations (39). CO triggers an intracellular cGMP increase by activating soluble guanylate cyclase that is also activated by nitric oxide (40). Moreover, previous studies have confirmed that CO-mediated antioxidative and anti-inflammatory properties operate through a guanylyl cyclase-dependent cGMP/PKG signaling pathway. Here we showed that CO suppresses PRRSV infection via the cGMP/PKG-dependent cascade, since treatment with either ODQ or KT5823 could reverse the inhibitory effect of CORM-2 on PRRSV infection (Fig. 8A to C). Moreover, PRRSV infection was decreased by incubation with 8-Br-cGMP, a cGMP analog (Fig. 8D to F). Our results are in accordance with a published report demonstrating that CO diminishes EV71 replication through the cGMP/PKG pathway (24). However, additional mechanisms underlying the cGMP-PKG axis suppression of PRRSV replication are not known. In fact, several mechanisms have been proposed to explain the antiviral effect of the cGMP/PKG signaling pathway. In EV71-infected SK-N-SH cells, CO caused a cGMP/PKG pathway-dependent inhibition of NADPH oxidase/reactive oxygen species (ROS) production, leading to the suppression of EV71 replication (24). Nevertheless, according to previous studies, ROS did not seem to be involved in the inhibition of PRRSV replication (41). We speculate that the inhibitory effect of cGMP-PKG on PRRSV replication may be mediated by mechanisms not included in our experimental model.

NF- $\kappa$ B, the foremost transcription factor that mediates the immunological inflammatory response, can be activated by LPS or virus infection or by induction of the expression of certain viral genes. Moreover, NF- $\kappa$ B is an attractive host target exploited by invading viruses to control cellular functions and regulate cellular metabolic events

(42). Although NF- $\kappa$ B has long been considered a key transcription factor for the expression of a variety of antiviral cytokines (43), some pathogens redirect the activity of NF- $\kappa$ B to become a virus-supportive function (44, 45). For example, influenza viruses replicated to high titers in cells containing preactivated NF- $\kappa$ B; conversely, progeny virus production was reduced when the NF- $\kappa$ B signaling pathway was blocked (46, 47). Williams et al. reported that sustained activation of NF- $\kappa$ B is required for the efficient expression of latent HIV type 1 (48). However, research results regarding the interplay between PRRSV and the NF- $\kappa$ B pathway have also been somewhat controversial. Lee and Kleiboeker (41) demonstrated that PRRSV infection activated NF- $\kappa$ B signaling in MARC-145 cells and PAMs involving I $\kappa$ B degradation and p65 nuclear translocation. In this study, we found that CO suppressed NF- $\kappa$ B activation in PRRSV-infected MARC-145 cells and PAMs through both inhibition of I $\kappa$ B degradation and p65 nuclear translocation. Meanwhile, our data also demonstrated that CO decreased NF- $\kappa$ B activation in LPS-treated cells, suggesting that the reduction of NF- $\kappa$ B activation in PRRSV-infected cells by CO was not due to the reduction of virus infection. Earlier studies showed that persistent activation of NF- $\kappa$ B appears to be a general response to PRRSV infection (41). The results in our study showed that PRRSV infection led to NF- $\kappa$ B activation, which is weakened by CORM-2 treatment. We therefore speculate that CO suppresses PRRSV infection through attenuation of the NF- $\kappa$ B pathway activation. Further studies showed that the optimal replication of PRRSV also depends on the activation of NF- $\kappa$ B (Fig. 11A to D), which is in good accordance with previous reports demonstrating that suppression of the NF- $\kappa$ B signaling pathway could block PRRSV replication (49). Although CO interference in NF- $\kappa$ B activation appears to be a pivotal event toward achieving the antiviral effect, the exact mechanism and molecular targets of this effect are not entirely clear. Therefore, although further studies are needed to explore the role of NF- $\kappa$ B in PRRSV infection, we can conclude that CO indeed abolishes PRRSV infection, either wholly or in part, by blocking NF- $\kappa$ B pathway activation.

PRRSV infection induces the release of proinflammatory factors, which may contribute to pathogenesis and inflammatory responses (50–52). Numerous studies have demonstrated that CO exhibits a potent anti-inflammatory effect in the pathogenesis of various diseases by modulating inflammatory cytokine production (53–56). Chhikara et al. demonstrated that CO reduces LPS-induced IL-8 and IL-1 $\beta$  expression in human monocytes (53). Megias et al. reported that CORM-2 inhibits proinflammatory cytokines IL-6 and IL-8 after cytokine induction in Caco-2 cells (55). In our study, we found that IL-6, IL-8, TNF- $\alpha$ , and IL-1 $\beta$  were significantly diminished by CO in PRRSV-infected MARC-145 cells and PAMs, suggesting that CO moderates PRRSV-induced inflammatory responses associated with viral replication. Collectively, these data demonstrate that CO inhibits inflammatory responses in PRRSV-infected cells by decreasing the mRNA levels of proinflammatory cytokines.

In summary, the results of this study demonstrate that CO, one of the HO-1 metabolites, exerts an anti-PRRSV effect by activating the cellular cGMP/PKG signaling pathway and negatively regulating cellular NF- $\kappa$ B signaling. Furthermore, CO exerts significant anti-inflammatory properties during PRRSV infection. These findings not only provide new insights into the molecular mechanism of HO-1 inhibition of PRRSV replication but also suggest potential new measures for controlling PRRSV infection.

## MATERIALS AND METHODS

**Cells, viruses, and reagents.** MARC-145 cells derived from African green monkey kidney cells were maintained in Dulbecco's modified Eagle's medium (DMEM; Life Technologies Corp., Grand Island, NY, USA) supplemented with 10% fetal bovine serum (FBS) and penicillin-streptomycin (Life Technologies Corp.). CRL2843 cells, a porcine alveolar macrophage line, were maintained in RPMI 1640 medium supplemented with 10% FBS and penicillin-streptomycin. SK-N-SH cells purchased from the China Center for Type Culture Collection (CCTCC) were maintained in DMEM supplemented with 10% FBS and penicillin-streptomycin. Porcine alveolar macrophages (PAMs) were obtained from healthy 6-week-old crossbred weaned (Landrace  $\times$  Yorkshire) PRRSV-negative pigs by use of a lung lavage technique as previously described (57) and maintained in RPMI 1640 medium supplemented with 10% FBS and penicillin-streptomycin. All cells were cultured and maintained at 37°C with 5% CO<sub>2</sub>. All animal work was done in strict accordance with the guidelines of the Institutional Animal Care and Use Committee and

**TABLE 1** Sequences of the primers used for qPCR

Primer	Sequence (5'–3')
PRRSV ORF7 gene	Forward, AGATCATCGCCCAACAAAAC Reverse, GACACAATTGCCGCTCACTA
PRRSV NSP2 gene	Forward, GTGGGTCGGCACCAGTT Reverse, GACGCAGACAAATCCAGAGG
$\beta$ -Actin	Forward, TCCCTGGAGAAGAGCTACGA Reverse, AGCACTGTGTTGGCGTACAG
mIL-6	Forward, AGAGGCACTGGCAGAAAAC Reverse, TGCAGGAAGTGGATCAGGAC
mIL-8	Forward, AGGACAAGAGCCAGGAAGAA Reverse, ACTGCACCTTCACACAGAGC
mTNF- $\alpha$	Forward, TCTGTCTGCTGCACCTTGGAGTGA Reverse, TTGAGGGTTTGCTACAACATGGGC
mIL-1 $\beta$	Forward, GGAAGACAAATTGCATGG Reverse, CCCAAGTGGTACATCAGCAC
pIL-6	Forward, AATGTCGAGGCTGTGCAGATT Reverse, TGGTGGCTTTGTCTGGATTCT
pIL-8	Forward, CACTGTGAAAATTCAGAAATCATTGTTA Reverse, CTCACAAATACCTGCACAACCTTC
pTNF- $\alpha$	Forward, TGGTGGTGCCGACAGATGG Reverse, GGCTGATGGTGTGAGTGAGGAA
pIL-1 $\beta$	Forward, ACCTGGACCTTGGTTCTCTG Reverse, CATCTGCCTGATGCTCTTGT
hVP1	Forward, CTGGTAAAGGTCCAGCACTC Reverse, GGGAGGTCTATCTCTCCAAC

approved by the Animal Care and Use Committee of Northwest A&F University, Yangling, Shaanxi Province, China.

The highly pathogenic PRRSV GD-HD strain (GenBank accession no. KP793736) was used for all experiments and is the strain represented by "PRRSV" in this article unless otherwise specified. For some experiments, PRRSV strains JXA1 and VR-2332 were also used but are specifically mentioned by name if used. Highly pathogenic PRRSV strain JXA1 was isolated from the pig farm at the source of an atypical PRRS outbreak in Jiangxi Province, China, in 2006 (GenBank accession no. EF112445); the classical PRRSV strain VR-2332 is the prototypical North American type 2 isolate (GenBank accession no. EF442771). Viruses were propagated, titrated in MARC-145 cells, and stored at  $-80^{\circ}\text{C}$ . Human enterovirus 71 (EV71) was purchased from the CCTCC.

Protoporphyrin IX cobalt chloride (CoPP; a classical inducer of HO-1 gene expression), tricarbonyl-dichlororuthenium (II) dimer  $\{[\text{Ru}(\text{CO})_3\text{Cl}_2]_2$ ; CORM-2, a transition metal carbonyl, can liberate CO to elicit direct biological activities), hemoglobin (Hb), and the cGMP analog 8-Br-cGMP were purchased from Sigma (St. Louis, MO, USA). The NF- $\kappa$ B inhibitor (BAY11-7082), sGC inhibitor (ODQ), and PKG inhibitor (KT5823) were obtained from Beyotime Biotechnology (Beyotime, Shanghai, China). Inactive CORM-2 (iCORM-2) was prepared by incubating CORM-2 dissolved in DMSO for 24 h at  $37^{\circ}\text{C}$  in a 5%  $\text{CO}_2$  humidified atmosphere to liberate CO.

**Quantitative reverse transcriptase PCR (qRT-PCR).** Total RNA was extracted from cells or supernatants using TRIzol reagent (Invitrogen, Carlsbad, CA, USA) and reverse transcribed using a Primescript RT reagent kit (TaKaRa, Dalian, China) according to the manufacturer's instructions. Quantitative PCRs (qPCRs) were performed using the StepOne Plus real-time PCR system (Applied Biosystems, Foster City, CA, USA) and FastStart Universal SYBR green master (Roche, Basel, Switzerland); reactions were performed in a  $10\text{-}\mu\text{l}$  volume.  $\beta$ -Actin mRNA was used as an internal control. The primers used for qPCR amplification are listed in Table 1.

For PRRSV RNA detection in supernatants, a plasmid containing a 372-bp fragment of the PRRSV ORF7 sequence was used to generate a standard curve. The standard curve was plotted from the results of parallel PCRs performed on serial dilutions of standard DNA. Absolute quantities of supernatant RNA were calculated by normalization to the standard curve.

**Western blot analysis.** Western blotting was performed as described previously (17) with the following modifications. Cells were harvested and lysed in NP-40 lysis buffer (Beyotime, Shanghai, China)

supplemented with protease and phosphatase inhibitors. For p65 nuclear translocation detection, nuclear and cytoplasmic protein samples were extracted using a nuclear/cytoplasmic fractionation kit (Beyotime). The cellular proteins were probed with one of the following primary antibodies: anti-PRRSV N protein antibody 6D10 at a 1:2,000 dilution (15), anti-I $\kappa$ B- $\alpha$  at a 1:1,000 dilution, anti-p-I $\kappa$ B- $\alpha$  at a 1:1,000 dilution, anti-p65 at a 1:1,000 dilution (Cell Signaling Technology, Danvers, MA, USA), anti-HO-1 at a 1:1,000 dilution (15), anti-histone 3 at a 1:1,000 dilution (Santa Cruz Biotechnology, Dallas, TX, USA), anti- $\alpha$ -tubulin at a 1:5,000 dilution (Sigma), or anti-VP1 at a 1:1,000 dilution (Abcam, Cambridge, United Kingdom). Horseradish peroxidase (HRP)-conjugated goat anti-mouse IgG at a 1:2,000 dilution (Jackson ImmunoResearch, West Grove, PA, USA) was used as the secondary antibody. The reactions were visualized using ECL reagent (Pierce, Rockford, IL, USA).

**PRRSV entry assay.** PRRSV entry assays were performed as previously described with the following modifications (58, 59). MARC-145 cells were initially challenged with PRRSV at an MOI of 0.1 for 2 h at 4°C. After the cells were rinsed three times with ice-cold PBS, they were cultured at 37°C in the presence of various concentrations of CORM-2 for 6 h. CORM-2 was added at 0, 2, or 4 h after the temperature shift (the time point at which the cells were switched to 37°C was set to 0 h). The cells were then rinsed three times with PBS and incubated for another 24 h at 37°C. The supernatants were harvested for virus titration, and the cells were collected for Western blot analysis.

**Neutralization assay.** The PRRSV-neutralizing assay was performed as previously described with the following modifications (60, 61). A 2-fold dilution of the hyperimmune serum sample was prepared in a 96-well plate (100  $\mu$ l/well). PRRSV (200 TCID<sub>50</sub>, 100  $\mu$ l/well) was added to mix with the hyperimmune serum sample and then incubated for 1 h at 37°C. After incubation, the serum-virus mixture was transferred onto 80% confluent MARC-145 cells that had been plated 24 h previously. At 24 h after PRRSV infection, the cells were fixed using 75% ethanol at 4°C for 30 min. Fixed cells were stained with PRRSV N protein antibody 6D10. After three washings with PBS, the cells were incubated with Alexa Fluor 488-conjugated goat anti-mouse IgG(H+L) (Invitrogen) as the secondary antibody for 1 h at 37°C. Nuclei were stained with DAPI (4',6-diamidino-2-phenylindole). Immunofluorescence was observed using a fluorescence microscope (model AF6000; Leica, Wetzlar, Germany). A serum sample from uninfected pigs was included in the assay as a control. The serum dilution that caused greater than 90% inhibition of virus infection was used in the following experiments to determine the effect of CO on intercellular spreading of the virus. In the virus spread assay, MARC-145 cells were infected with PRRSV at a TCID<sub>50</sub> of 200. After incubation at 37°C for 3 h to allow virus entry into cells, PRRSV-infected cells were treated with hyperimmune serum with a definite virus-neutralizing titer plus CORM-2 or hyperimmune serum only. At 24, 36, and 48 hpi, the cells were fixed, stained with specific antibodies as described above, and analyzed with a fluorescence microscope (Leica AF6000). Cell culture supernatants were harvested at 24, 36, and 48 hpi, and virus titers were determined by TCID<sub>50</sub> assay.

**ELISA.** As Hb has a very high affinity for CO, the levels of CO released by host cells after PRRSV infection were measured by detecting the HbCO content using commercially available HbCO enzyme-linked immunosorbent assay (ELISA) kits (Elabscience Biotechnology, Wuhan, China) according to the manufacturer's instructions. The process is briefly described as follows: MARC-145 cells were seeded in 6-well plates at a density of  $2 \times 10^5$  cells/well. Twenty-four hours later, the cells were infected with PRRSV at an MOI of 0.1 and incubated at 37°C for 1 h. After the cells were washed with PBS three times, 3% FBS plus DMEM containing 50  $\mu$ g/ml Hb was added. Supernatants were harvested at 24, 36, and 48 hpi for ELISA to quantify the HbCO levels as a measure of CO production. To determine the relationship between CO production and PRRSV dose, MARC-145 cells were infected with PRRSV at an MOI of 0.1, 0.5, or 1 and then treated with Hb (50  $\mu$ g/ml) from 1 hpi onward. At 24 hpi, supernatants were harvested to quantify the levels of HbCO by ELISA as a measure of CO production. The absorbance was detected at 450 nm using an Epoch microplate spectrophotometer (BioTek Instruments, Winooski, VT, USA). PRRSV-mock-infected MARC-145 cells were included as a control in the analysis.

**Inhibition of signaling pathway transduction.** MARC-145 or PAMs were pretreated with DMSO either alone or with the NF- $\kappa$ B inhibitor BAY11-7082 (2.5 to 10  $\mu$ M) for 1 h, washed with PBS three times, and then infected with PRRSV at an MOI of 0.1 in the absence of inhibitor. After 36 h, the cells were harvested to detect N protein expression by using Western blotting and supernatants were harvested to assess virus production by virus titration.

MARC-145 cells were seeded into 24-well plates, and 24 h later, the cells were infected with PRRSV at an MOI of 0.1. After 1 h, the supernatants were discarded, following three washes with PBS, and 3% FBS plus DMEM with or without a definite concentration of CORM-2 (100  $\mu$ M) and the sGC-specific inhibitor ODQ (10  $\mu$ M) or the PKG-specific inhibitor KT5823 (1  $\mu$ M) was added. After 36 h, supernatants were harvested for virus copy number determinations using qPCR and cells were harvested for PRRSV ORF7 mRNA and N protein expression detection using qPCR and Western blotting, respectively.

**IFA.** An indirect immunofluorescence assay (IFA) was performed as previously described (62) with the following modifications. MARC-145 cells were infected with PRRSV at an MOI of 0.1, followed by treatment with various concentrations of CORM-2 or iCORM-2 from 1 hpi onward. At 24 hpi, the cells were fixed with 75% ethanol at 4°C for 30 min. Following three washes with PBS, the fixed cells were incubated with monoclonal antibodies (6D10) against PRRSV N protein at 37°C for 1 h. After three washes with PBS, the cells were incubated with Alexa Fluor 488-conjugated goat anti-mouse IgG (H+L) (Invitrogen) as the secondary antibody for 1 h at 37°C. Nuclei were stained with DAPI. Immunofluorescence was observed using a fluorescence microscope (Leica AF6000). Mock-infected cells were used as controls to establish background staining levels.

**Luciferase reporter assay.** The luciferase reporter assay was performed as described previously (17) with the following modifications. MARC-145 cells and CRL2843 cells were seeded into 24-well plates at



a density of  $0.5 \times 10^5$  cells/well. After incubation for 16 h, the cells were transfected with 100 ng/well of pNF- $\kappa$ B-Luc and 50 ng/well of pRL-TK using X-tremeGENE HP DNA transfection reagent (Roche, Mannheim, Germany). pRL-TK plasmid was used as an internal control for transfection efficiency. At 12 h posttransfection, MARC-145 cells were infected with PRRSV at an MOI of 0.1, followed by treatment with various concentrations of CORM-2 or a single concentration of iCORM-2 from 1 hpi onward. Similarly, 12 h after transfection, CRL2843 cells were treated with lipopolysaccharide (LPS) in the presence of various doses of CORM-2 or 150  $\mu$ M iCORM-2. At 36 h after PRRSV infection or LPS treatment, the cells were harvested for determination of firefly luciferase and *Renilla* luciferase activities on a Synergy HT multi-mode microplate reader (BioTek, Winooski, VT) using the Dual-Luciferase reporter assay system (Promega, Madison, WI, USA) according to the manufacturer's instructions.

**Virus titration.** Virus progeny production was determined by titration as previously described (63) with minor modifications. MARC-145 cells were trypsinized and seeded into a 96-well plate 24 h before virus infection. Virus supernatants were prepared by serial dilution, and 100- $\mu$ l volumes of the dilutions were added per well in replicates of eight. Six days after infection, the TCID<sub>50</sub> was calculated using the Reed-Muench method.

**Statistical analysis.** All experiments were performed with at least three independent replicates. The results were analyzed using Student's *t* test if two groups were compared and one-way analysis of variance (64) if three or more groups were tested against a control group. A *P* value of <0.05 was considered to indicate statistical significance.

## ACKNOWLEDGMENTS

This study was supported by the National Natural Science Foundation of China (grant no. 31472173 and 31430084), the Natural Science Basic Research Plan in Shaanxi Province of China (grant no. 2014JQ3088), the Northwest A&F University talent special fund (grant no. Z111021201), and the Fundamental Research Fund (grant no. 2452016046).

## REFERENCES

- Albina E. 1997. Epidemiology of porcine reproductive and respiratory syndrome (PRRS): an overview. *Vet Microbiol* 55:309–316. [https://doi.org/10.1016/S0378-1135\(96\)01322-3](https://doi.org/10.1016/S0378-1135(96)01322-3).
- Cavanagh D. 1997. Nidovirales: a new order comprising Coronaviridae and Arteriviridae. *Arch Virol* 142:629–633.
- Pejsak Z, Stadejek T, Markowska-Daniel I. 1997. Clinical signs and economic losses caused by porcine reproductive and respiratory syndrome virus in a large breeding farm. *Vet Microbiol* 55:317–322. [https://doi.org/10.1016/S0378-1135\(96\)01326-0](https://doi.org/10.1016/S0378-1135(96)01326-0).
- Darwich L, Diaz I, Mateu E. 2010. Certainties, doubts and hypotheses in porcine reproductive and respiratory syndrome virus immunobiology. *Virus Res* 154:123–132. <https://doi.org/10.1016/j.virusres.2010.07.017>.
- Meng XJ. 2000. Heterogeneity of porcine reproductive and respiratory syndrome virus: implications for current vaccine efficacy and future vaccine development. *Vet Microbiol* 74:309–329. [https://doi.org/10.1016/S0378-1135\(00\)00196-6](https://doi.org/10.1016/S0378-1135(00)00196-6).
- Murtaugh MP, Stadejek T, Abraham JE, Lam TT, Leung FC. 2010. The ever-expanding diversity of porcine reproductive and respiratory syndrome virus. *Virus Res* 154:18–30. <https://doi.org/10.1016/j.virusres.2010.08.015>.
- Calzada-Nova G, Schnitzlein WM, Husmann RJ, Zuckermann FA. 2011. North American porcine reproductive and respiratory syndrome viruses inhibit type I interferon production by plasmacytoid dendritic cells. *J Virol* 85:2703–2713. <https://doi.org/10.1128/JVI.01616-10>.
- Kimman TG, Cornelissen LA, Moormann RJ, Rebel JM, Stockhofe-Zurwieden N. 2009. Challenges for porcine reproductive and respiratory syndrome virus (PRRSV) vaccinology. *Vaccine* 27:3704–3718. <https://doi.org/10.1016/j.vaccine.2009.04.022>.
- Yoo D, Song C, Sun Y, Du Y, Kim O, Liu HC. 2010. Modulation of host cell responses and evasion strategies for porcine reproductive and respiratory syndrome virus. *Virus Res* 154:48–60. <https://doi.org/10.1016/j.virusres.2010.07.019>.
- Chung SW, Hall SR, Perrella MA. 2009. Role of haem oxygenase-1 in microbial host defence. *Cell Microbiol* 11:199–207. <https://doi.org/10.1111/j.1462-5822.2008.01261.x>.
- Devadas K, Dhawan S. 2006. Hemin activation ameliorates HIV-1 infection via heme oxygenase-1 induction. *J Immunol* 176:4252–4257. <https://doi.org/10.4049/jimmunol.176.7.4252>.
- Hill-Batorski L, Halfmann P, Neumann G, Kawaoka Y. 2013. The cytoprotective enzyme heme oxygenase-1 suppresses Ebola virus replication. *J Virol* 87:13795–13802. <https://doi.org/10.1128/JVI.02422-13>.
- Protzer U, Seyfried S, Quasdorff M, Sass G, Svorcova M, Webb D, Bohne F, Hosel M, Schirmacher P, Tiegs G. 2007. Antiviral activity and hepatoprotection by heme oxygenase-1 in hepatitis B virus infection. *Gastroenterology* 133:1156–1165. <https://doi.org/10.1053/j.gastro.2007.07.021>.
- Zhu Z, Wilson AT, Mathahs MM, Wen F, Brown KE, Luxon BA, Schmidt WN. 2008. Heme oxygenase-1 suppresses hepatitis C virus replication and increases resistance of hepatocytes to oxidant injury. *Hepatology* 48:1430–1439. <https://doi.org/10.1002/hep.22491>.
- Xiao S, Zhang A, Zhang C, Ni H, Gao J, Wang C, Zhao Q, Wang X, Wang X, Ma C, Liu H, Li N, Mu Y, Sun Y, Zhang G, Hiscox JA, Hsu WH, Zhou EM. 2014. Heme oxygenase-1 acts as an antiviral factor for porcine reproductive and respiratory syndrome virus infection and over-expression inhibits virus replication in vitro. *Antivir Res* 110:60–69. <https://doi.org/10.1016/j.antiviral.2014.07.011>.
- Zhang C, Pu F, Zhang A, Xu L, Li N, Yan Y, Gao J, Liu H, Zhang G, Goodfellow IG, Zhou EM, Xiao S. 2015. Heme oxygenase-1 suppresses bovine diarrhoea virus replication in vitro. *Sci Rep* 5:15575. <https://doi.org/10.1038/srep15575>.
- Xiao S, Wang X, Ni H, Li N, Zhang A, Liu H, Pu F, Xu L, Gao J, Zhao Q, Mu Y, Wang C, Sun Y, Du T, Xu X, Zhang G, Hiscox JA, Goodfellow IG, Zhou EM. 2015. MiR-24-3p promotes porcine reproductive and respiratory syndrome virus replication through suppression of heme oxygenase-1 expression. *J Virol* 89:4494–4503. <https://doi.org/10.1128/JVI.02810-14>.
- Tenhunen R, Marver HS, Schmid R. 1968. The enzymatic conversion of heme to bilirubin by microsomal heme oxygenase. *Proc Natl Acad Sci U S A* 61:748–755. <https://doi.org/10.1073/pnas.61.2.748>.
- Chung SW, Liu X, Macias AA, Baron RM, Perrella MA. 2008. Heme oxygenase-1-derived carbon monoxide enhances the host defense response to microbial sepsis in mice. *J Clin Invest* 118:239–247. <https://doi.org/10.1172/JCI32730>.
- Otterbein LE. 2002. Carbon monoxide: innovative anti-inflammatory properties of an age-old gas molecule. *Antioxid Redox Signal* 4:309–319. <https://doi.org/10.1089/152308602753666361>.
- Otterbein LE, Zuckerbraun BS, Haga M, Liu F, Song R, Usheva A, Stachulak C, Bodyak N, Smith RN, Csizmadia E, Tyagi S, Akamatsu Y, Flavell RJ, Billiar TR, Zeng E, Bach FH, Choi AM, Soares MP. 2003. Carbon monoxide suppresses arteriosclerotic lesions associated with chronic graft rejection and with balloon injury. *Nat Med* 9:183–190. <https://doi.org/10.1038/nm817>.
- Ryter SW, Choi AM. 2006. Therapeutic applications of carbon monoxide

- in lung disease. *Curr Opin Pharmacol* 6:257–262. <https://doi.org/10.1016/j.coph.2006.03.002>.
23. Verma A, Hirsch DJ, Glatt CE, Ronnett GV, Snyder SH. 1993. Carbon monoxide: a putative neural messenger. *Science* 259:381–384. <https://doi.org/10.1126/science.7678352>.
  24. Tung WH, Hsieh HL, Lee IT, Yang CM. 2011. Enterovirus 71 induces integrin beta1/EGFR-Rac1-dependent oxidative stress in SK-N-SH cells: role of HO-1/CO in viral replication. *J Cell Physiol* 226:3316–3329. <https://doi.org/10.1002/jcp.22677>.
  25. Desmard M, Davidge KS, Bouvet O, Morin D, Roux D, Foresti R, Ricard JD, Denamur E, Poole RK, Montravers P, Motterlini R, Boczkowski J. 2009. A carbon monoxide-releasing molecule (CORM-3) exerts bactericidal activity against *Pseudomonas aeruginosa* and improves survival in an animal model of bacteraemia. *FASEB J* 23:1023–1031. <https://doi.org/10.1096/fj.08-122804>.
  26. Nobre LS, Seixas JD, Romao CC, Saraiva LM. 2007. Antimicrobial action of carbon monoxide-releasing compounds. *Antimicrob Agents Chemother* 51:4303–4307. <https://doi.org/10.1128/AAC.00802-07>.
  27. Kanagawa F, Takahashi T, Inoue K, Shimizu H, Omori E, Morimatsu H, Maeda S, Katayama H, Nakao A, Morita K. 2010. Protective effect of carbon monoxide inhalation on lung injury after hemorrhagic shock/resuscitation in rats. *J Trauma* 69:185–194. <https://doi.org/10.1097/TA.0b013e3181bbd516>.
  28. Kawanishi S, Takahashi T, Morimatsu H, Shimizu H, Omori E, Sato K, Matsumi M, Maeda S, Nakao A, Morita K. 2013. Inhalation of carbon monoxide following resuscitation ameliorates hemorrhagic shock-induced lung injury. *Mol Med Rep* 7:3–10. <https://doi.org/10.3892/mmr.2012.1173>.
  29. Maines MD. 1993. Carbon monoxide: an emerging regulator of cGMP in the brain. *Mol Cell Neurosci* 4:389–397. <https://doi.org/10.1006/mcne.1993.1049>.
  30. Maines MD. 1997. The heme oxygenase system: a regulator of second messenger gases. *Annu Rev Pharmacol Toxicol* 37:517–554. <https://doi.org/10.1146/annurev.pharmtox.37.1.517>.
  31. Morita T, Perrella MA, Lee ME, Kourembanas S. 1995. Smooth-muscle cell-derived carbon-monoxide is a regulator of vascular cGMP. *Proc Natl Acad Sci U S A* 92:1475–1479. <https://doi.org/10.1073/pnas.92.5.1475>.
  32. Wegener JW, Nawrath H, Wolfsgruber W, Kuhbandner S, Werner C, Hofmann F, Feil R. 2002. cGMP-dependent protein kinase I mediates the negative inotropic effect of cGMP in the murine myocardium. *Circ Res* 90:18–20. <https://doi.org/10.1161/hh102.103222>.
  33. Li YY, Gao C, Shi YR, Tang YH, Liu L, Xiong T, Du M, Xing MY, Liu LG, Yao P. 2013. Carbon monoxide alleviates ethanol-induced oxidative damage and inflammatory stress through activating p38 MAPK pathway. *Toxicol Appl Pharmacol* 273:53–58. <https://doi.org/10.1016/j.taap.2013.08.019>.
  34. Davidge KS, Sanguinetti G, Yee CH, Cox AG, McLeod CW, Monk CE, Mann BE, Motterlini R, Poole RK. 2009. Carbon monoxide-releasing antibacterial molecules target respiration and global transcriptional regulators. *J Biol Chem* 284:4516–4524. <https://doi.org/10.1074/jbc.M808210200>.
  35. Desmard M, Foresti R, Morin D, Dagouassat M, Berdeau A, Denamur E, Crook SH, Mann BE, Scapens D, Montravers P, Boczkowski J, Motterlini R. 2012. Differential antibacterial activity against *Pseudomonas aeruginosa* by carbon monoxide-releasing molecules. *Antioxid Redox Signal* 16:153–163. <https://doi.org/10.1089/ars.2011.3959>.
  36. Nobre LS, Al-Shahrour F, Dopazo J, Saraiva LM. 2009. Exploring the antimicrobial action of a carbon monoxide-releasing compound through whole-genome transcription profiling of *Escherichia coli*. *Microbiology* 155:813–824. <https://doi.org/10.1099/mic.0.023911-0>.
  37. Blancou P, Tardif V, Simon T, Remy S, Carreno L, Kalergis A, Anegon I. 2011. Immunoregulatory properties of heme oxygenase-1. *Methods Mol Biol* 677:247–268. [https://doi.org/10.1007/978-1-60761-869-0\\_18](https://doi.org/10.1007/978-1-60761-869-0_18).
  38. Remy S, Blancou P, Tesson L, Tardif V, Brion R, Royer PJ, Motterlini R, Foresti R, Painchaud M, Pogu S, Gregoire M, Bach JM, Anegon I, Chauveau C. 2009. Carbon monoxide inhibits TLR-induced dendritic cell immunogenicity. *J Immunol* 182:1877–1884. <https://doi.org/10.4049/jimmunol.0802436>.
  39. Ghosh S, Gal J, Marczin N. 2010. Carbon monoxide: endogenous mediator, potential diagnostic and therapeutic target. *Ann Med* 42:1–12. <https://doi.org/10.3109/07853890903482877>.
  40. Siow RC, Sato H, Mann GE. 1999. Heme oxygenase-carbon monoxide signalling pathway in atherosclerosis: anti-atherogenic actions of bilirubin and carbon monoxide? *Cardiovasc Res* 41:385–394. [https://doi.org/10.1016/S0008-6363\(98\)00278-8](https://doi.org/10.1016/S0008-6363(98)00278-8).
  41. Lee SM, Kleiboecker SB. 2005. Porcine arterivirus activates the NF-kappaB pathway through IkappaB degradation. *Virology* 342:47–59. <https://doi.org/10.1016/j.virol.2005.07.034>.
  42. Amici C, Rossi A, Ciafre S, Marinaro B, Balsamo M, Levrero M, Santoro MG. 2006. Herpes simplex virus disrupts NF-kappaB regulation by blocking its recruitment on the IkappaBalpha promoter and directing the factor on viral genes. *J Biol Chem* 281:7110–7117. <https://doi.org/10.1074/jbc.M512366200>.
  43. Hayden MS, Ghosh S. 2008. Shared principles in NF-kappaB signaling. *Cell* 132:344–362. <https://doi.org/10.1016/j.cell.2008.01.020>.
  44. Asamitsu K, Yamaguchi T, Nakata K, Hibi Y, Victoriano AF, Imai K, Onozaki K, Kitade Y, Okamoto T. 2008. Inhibition of human immunodeficiency virus type 1 replication by blocking IkappaB kinase with noraristeromycin. *J Biochem* 144:581–589. <https://doi.org/10.1093/jb/mvn104>.
  45. Ludwig S, Planz O. 2008. Influenza viruses and the NF-kappaB signaling pathway—towards a novel concept of antiviral therapy. *Biol Chem* 389:1307–1312. <https://doi.org/10.1515/BC.2008.148>.
  46. Nimmerjahn F, Dudziak D, Dirmeier U, Hobom G, Riedel A, Schlee M, Staudt LM, Rosenwald A, Behrens U, Bornkamm GW, Mautner J. 2004. Active NF-kappaB signalling is a prerequisite for influenza virus infection. *J Gen Virol* 85:2347–2356. <https://doi.org/10.1099/vir.0.79958-0>.
  47. Wurzer WJ, Ehrhardt C, Pleschka S, Berberich-Siebelt F, Wolff T, Walczak H, Planz O, Ludwig S. 2004. NF-kappaB-dependent induction of tumor necrosis factor-related apoptosis-inducing ligand (TRAIL) and Fas/FasL is crucial for efficient influenza virus propagation. *J Biol Chem* 279:30931–30937. <https://doi.org/10.1074/jbc.M403258200>.
  48. Williams SA, Kwon H, Chen LF, Greene WC. 2007. Sustained induction of NF-kappa B is required for efficient expression of latent human immunodeficiency virus type 1. *J Virol* 81:6043–6056. <https://doi.org/10.1128/JVI.02074-06>.
  49. Wang D, Cao L, Xu Z, Fang L, Zhong Y, Chen Q, Luo R, Chen H, Li K, Xiao S. 2013. MiR-125b reduces porcine reproductive and respiratory syndrome virus replication by negatively regulating the NF-kappaB pathway. *PLoS One* 8:e55838. <https://doi.org/10.1371/journal.pone.0055838>.
  50. Lunney JK, Fritz ER, Reecy JM, Kuhar D, Prucnal E, Molina R, Christopher-Hennings J, Zimmerman J, Rowland RR. 2010. Interleukin-8, interleukin-1beta, and interferon-gamma levels are linked to PRRS virus clearance. *Viral Immunol* 23:127–134. <https://doi.org/10.1089/vim.2009.0087>.
  51. Sipos W, Duvigneau C, Pietschmann P, Holler K, Hartl R, Wahl K, Steinborn R, Gemeiner M, Willheim M, Schmoll F. 2003. Parameters of humoral and cellular immunity following vaccination of pigs with a European modified-live strain of porcine reproductive and respiratory syndrome virus (PRRSV). *Viral Immunol* 16:335–346. <https://doi.org/10.1089/088282403322396136>.
  52. Thanawongnuwech R, Thacker B, Halbur P, Thacker EL. 2004. Increased production of proinflammatory cytokines following infection with porcine reproductive and respiratory syndrome virus and *Mycoplasma hyopneumoniae*. *Clin Diagn Lab Immunol* 11:901–908.
  53. Chhikara M, Wang S, Kern SJ, Ferreyra GA, Barb JJ, Munson PJ, Danner RL. 2009. Carbon monoxide blocks lipopolysaccharide-induced gene expression by interfering with proximal TLR4 to NF-kappaB signal transduction in human monocytes. *PLoS One* 4:e8139. <https://doi.org/10.1371/journal.pone.0008139>.
  54. Mazzola S, Forni M, Albertini M, Bacci ML, Zannoni A, Gentilini F, Lavitrano M, Bach FH, Otterbein LE, Clement MG. 2005. Carbon monoxide pretreatment prevents respiratory derangement and ameliorates hyperacute endotoxic shock in pigs. *FASEB J* 19:2045–2047.
  55. Megias J, Busserolles J, Alcaraz MJ. 2007. The carbon monoxide-releasing molecule CORM-2 inhibits the inflammatory response induced by cytokines in Caco-2 cells. *Br J Pharmacol* 150:977–986.
  56. Motterlini R, Haas B, Foresti R. 2012. Emerging concepts on the anti-inflammatory actions of carbon monoxide-releasing molecules (CO-RMs). *Med Gas Res* 2:28. <https://doi.org/10.1186/2045-9912-2-28>.
  57. Wensvoort G, Terpstra C, Pol JM, ter Laak EA, Bloemraad M, de Kluyver EP, Kragten C, van Buiten L, den Besten A, Wagenaar F. 1991. Mystery swine disease in The Netherlands: the isolation of Lelystad virus. *Vet Q* 13:121–130. <https://doi.org/10.1080/01652176.1991.9694296>.
  58. Hong W, Li T, Song Y, Zhang R, Zeng Z, Han S, Zhang X, Wu Y, Li W, Cao Z. 2014. Inhibitory activity and mechanism of two scorpion venom peptides against herpes simplex virus type 1. *Antivir Res* 102:1–10. <https://doi.org/10.1016/j.antiviral.2013.11.013>.
  59. Yang Q, Gao L, Si J, Sun Y, Liu J, Cao L, Feng WH. 2013. Inhibition of porcine reproductive and respiratory syndrome virus replication by flavaspicid acid AB. *Antivir Res* 97:66–73. <https://doi.org/10.1016/j.antiviral.2012.11.004>.

60. Guo R, Katz BB, Tomich JM, Gallagher T, Fang Y. 2016. Porcine reproductive and respiratory syndrome virus utilizes nanotubes for intercellular spread. *J Virol* 90:5163–5175. <https://doi.org/10.1128/JVI.00036-16>.
61. Yoon IJ, Joo HS, Goyal SM, Molitor TW. 1994. A modified serum neutralization test for the detection of antibody to porcine reproductive and respiratory syndrome virus in swine sera. *J Vet Diagn Invest* 6:289–292.
62. Liu H, Wang Y, Duan H, Zhang A, Liang C, Gao J, Zhang C, Huang B, Li Q, Li N, Xiao S, Zhou EM. 2015. An intracellularly expressed Nsp9-specific nanobody in MARC-145 cells inhibits porcine reproductive and respiratory syndrome virus replication. *Vet Microbiol* 181:252–260. <https://doi.org/10.1016/j.vetmic.2015.10.021>.
63. Xiao S, Wang Q, Gao J, Wang L, He Z, Mo D, Liu X, Chen Y. 2011. Inhibition of highly pathogenic PRRSV replication in MARC-145 cells by artificial microRNAs. *Virology* 422:488–491. <https://doi.org/10.1016/j.virol.2011.08.011>.
64. Casanova-Salas I, Masia E, Arminan A, Calatrava A, Mancarella C, Rubio-Briones J, Scotlandi K, Vicent MJ, Lopez-Guerrero JA. 2015. MiR-187 targets the androgen-regulated gene ALDH1A3 in prostate cancer. *PLoS One* 10:e0125576. <https://doi.org/10.1371/journal.pone.0125576>.